

論文 / 著書情報
Article / Book Information

Title(English)	Coefficient of earth pressure at-rest derived from the Sekiguchi-Ohta model
Authors(English)	Thirapong Pipatpongsa, Tomohide Takeyama, Hideki Ohta, Atsushi Iizuka
Citation(English)	Proceeding of the 16th Southeast Asian Geotechnical Conference, Vol. , No. , pp. 325-331
Pub. date	2007, 5

Coefficient of Earth Pressure At-Rest Derived from the Sekiguchi-Ohta Model

T. Pipatpongsa

Global Scientific Information and Computing Center, Tokyo Institute of Technology, Tokyo, Japan
pthira@gsic.titech.ac.jp

T. Takeyama¹ & H. Ohta²

Department of International Development Engineering, Tokyo Institute of Technology, Tokyo, Japan
¹takeyama@ide.titech.ac.jp, ²ohta@ide.titech.ac.jp

A. Iizuka

Research Center for Urban and Security, Kobe University, Kobe, Japan
iizuka@kobe-u.ac.jp

Abstract: This paper proposes a method suggesting the relationship between critical state parameter, M and coefficient of earth pressure at rest, K_o derived from the Sekiguchi-Ohta model (1977). Based on the fact that K_o condition existed on the discontinuous corner of the yield surface between active and passive yield loci, the slight interruption is undertaken upon numerically perturbing the state of stress at the K_o condition by small amount of balanced active and passive load increments. The resulting successive stress condition is, therefore, kept tracing and fluctuating along the K_o -consolidation axis whilst increasing a consolidated volume. The lateral strain increments obtained is expected to be zero if the K_o value suitable to the model is employed. Under this criterion, the theoretical K_o expression can be evaluated analytically as the expression solely related to M . It is found that the derived expression agrees well with the available published experimental data and empirical relations.

1 INTRODUCTION

1.1 K_o Expression

Many studies have derived the theoretical relation between K_o and critical state parameter, M based on critical state models (Roscoe *et al.*, 1963, Schofield & Wroth, 1968, Roscoe & Burland, 1968). However, the derived K_o expression tends to overestimate the empirical relationship (Wood, 1990). As a result, K_o , which specifies the starting state of stress of soil mass, still remains theoretically unaddressed in the great extent though it can favorably contribute to the quality of analyses in geotechnical engineering problems.

The Sekiguchi-Ohta model (Sekiguchi & Ohta, 1977) is the most popular anisotropic soil model used in Japan. It is recognized that the model possesses the singular corner on the yield surface where the state of virgin K_o -consolidation is placed. Unlike the corner of the original Cam clay which is located on the isotropic consolidation axis, the corner of the Sekiguchi-Ohta model is positioned on the K_o -consolidation axis. Nevertheless, there is no difficulty to handle these kinds of non-smooth yield surfaces. Recent research has provided the mathematical procedure to solve this obstacle (Pipatpongsa *et al.*, 2002).

The authors have proposed a method to derive K_o expression based on a purely frictional dissipation function regarded in both the original Cam clay model and the Sekiguchi-Ohta models (Pipatpongsa *et al.* 2001, Pipatpongsa *et al.*, in prep.). By this context, we can associate the non-zero plastic dissipation at the state on the apex yield surface with an averaged plastic flow of active and passive states. As a consequence, the theoretical K_o -value is formulated by energy-balanced equation. The derived expression

of K_o agreed well with a number of compiled experiment results and widely-used empirical relations. However, it is not clear what would suffer in analyses if the theoretically derived K_o is not precisely employed when K_o of subsoil data is required to input for FEM software package especially devised for the Sekiguchi-Ohta model.

Therefore, this paper aims to investigate the derived relationship of K_o expression for the Sekiguchi-Ohta model while providing a comprehensible illustration of the matter concerned. The study may settle the dilemma on whether K_o value should be treated as an independent parameter or as a dependent parameter for the model.

2 THEORETICAL APPROACH

2.1 K_o Condition

Under uni-axial loading condition, rate of strain in lateral direction is zero while rate of strain in axial direction is only appeared in strain rate tensor as shown by Eq. (1). To reduce the complexity due to tensor notation, terms of volumetric and deviatoric rate of strain expressed by Eq. (2) are mainly considered. Eq. (3) ascertains that the resulting strain rate ratio of deviatoric to volumetric part is 2/3 for this particular case:

$$\dot{\boldsymbol{\epsilon}} = \begin{bmatrix} \dot{\epsilon}_a & 0 & 0 \\ 0 & 0 & 0 \\ 0 & 0 & 0 \end{bmatrix} \quad (1)$$

$$\begin{Bmatrix} \dot{\epsilon}_v \\ \dot{\epsilon}_s \end{Bmatrix} = \begin{bmatrix} 1 & 2 \\ 2 & -2 \\ 3 & -3 \end{bmatrix} \cdot \begin{Bmatrix} \dot{\epsilon}_a \\ 0 \end{Bmatrix} = \begin{Bmatrix} 1 \\ 2 \\ 3 \end{Bmatrix} \dot{\epsilon}_a, \quad \frac{\dot{\epsilon}_s}{\dot{\epsilon}_v} = \frac{2}{3} \quad (2),(3)$$

Since K_o condition is defined in axi-symmetric condition where lateral stress is identical in radial direction, stress tensor and stress rate tensor can be expressed by Eqs. (4) and (5). Accordingly, state of stress and its rate form can be taken in form of mean and deviatoric parts expressed by Eqs. (6) and (7) where σ_a is referred to an axial stress.

$$\boldsymbol{\sigma} = \sigma_a \begin{bmatrix} 1 & 0 & 0 \\ 0 & K_o & 0 \\ 0 & 0 & K_o \end{bmatrix}, \quad \dot{\boldsymbol{\sigma}} = \dot{\sigma}_a \begin{bmatrix} 1 & 0 & 0 \\ 0 & K_o & 0 \\ 0 & 0 & K_o \end{bmatrix} \quad (4),(5)$$

$$\begin{Bmatrix} p \\ q \end{Bmatrix} = \begin{Bmatrix} \frac{1+2K_o}{3} \\ 1-K_o \end{Bmatrix} \sigma_a, \quad \begin{Bmatrix} \dot{p} \\ \dot{q} \end{Bmatrix} = \begin{Bmatrix} \frac{1+2K_o}{3} \\ 1-K_o \end{Bmatrix} \dot{\sigma}_a \quad (6),(7)$$

Usually, K_o is defined in terms of stress ratio between horizontal to vertical stress. The mean stress p and deviatoric stress q can be used to define K_o by referring the stress ratio η_o given in Eq. (8). For elastic part, the volumetric and deviatoric rate of strains are determined by Eqs. (9) and (10).

$$\eta_o = \frac{q_o}{p_o} = \frac{\dot{q}}{\dot{p}} = 3 \frac{1-K_o}{1+2K_o} \quad (8)$$

$$\frac{\dot{\epsilon}_v^e}{\dot{\epsilon}_s^e} = \frac{\dot{p}}{K}, \quad \frac{\dot{\epsilon}_s^e}{\dot{\epsilon}_v^e} = \frac{\dot{q}}{3G} \quad (9),(10)$$

where K is bulk modulus and G is shear modulus which are conveniently expressed in terms of critical state parameter M , coefficient of dilatancy D , compression index λ , swelling index κ , irreversibility ratio Λ , Poisson's ratio ν in expressions shown by Eqs. (11) to (15).

According to Eqs. (9) to (15), the ratio between elastic deviatoric strain rate to elastic volumetric strain rate is given in Eq. (16). By virtue of elastic response under K_o condition, the appropriate Poisson's ratio can be derived by equating Eq. (16) to $2/3$, then G/K ratio expressed by μ can be reduced to the particular relation given by Eq. (17) which is equivalent to a Poisson's ratio function given by Eq. (18) by means of Eq. (15).

$$K = \frac{p}{\kappa} (1+e_o) = \frac{\Lambda}{MD(1-\Lambda)} p, \quad G = \mu K \quad (11),(12)$$

$$\Lambda = 1 - \frac{\kappa}{\lambda}, \quad D = \frac{\lambda - \kappa}{(1+e_o)M}, \quad \mu = \frac{3}{2} \left(\frac{1-2\nu}{1+\nu} \right) \quad (13),(14),(15)$$

$$\frac{\dot{\epsilon}_s^e}{\dot{\epsilon}_v^e} = \frac{\dot{q}}{\dot{p}} \frac{K}{3G} = \frac{\eta_o}{3\mu} \quad (16)$$

$$\mu = \frac{\eta_o}{2}, \quad \nu = \frac{K_o}{1+K_o} \quad (17),(18)$$

2.2 Constitutive Model

The Ohta-Hata model (Ohta & Hata, 1971) is an original form of the Sekiguchi-Ohta model under axi-symmetric stress condition particularly. The mathematical point of discontinuity is found due to a turning sign given by an absolute function existed in the expression. The expression for Ohta-Hata yield function and time derivative are presented in Eqs.(19) and (20). The evolution law of hardening stress is given by Eq.(21). The consistency parameter γ shown by Eq.(23) is determined via flow rule Eqs.(22).

$$f = M \ln \left(\frac{p}{p_c} \right) + \left| \frac{q}{p} - \eta_o \right| = 0 \quad (19)$$

$$\dot{f} = \frac{\partial f}{\partial p} \dot{p} + \frac{\partial f}{\partial q} \dot{q} + \frac{\partial f}{\partial p_c} \dot{p}_c = 0 \quad (20)$$

$$\text{where } \dot{p}_c = \frac{p_c}{MD} \dot{\epsilon}_v^p, \quad \dot{\epsilon}_v^p = \gamma \frac{\partial f}{\partial p} \quad (21),(22)$$

$$\gamma = - \frac{\frac{\partial f}{\partial p} \dot{p} + \frac{\partial f}{\partial q} \dot{q}}{\frac{\partial f}{\partial p_c} \frac{p_c}{MD} \frac{\partial f}{\partial p}} \quad (23)$$

Eq. (19) can be dissociated into the active yield locus and passive yield locus shown by Eqs. (24) and (25) and plotted in Fig. 1. The subscript A and P denote active ($q/p > \eta_o$) state and passive state ($q/p < \eta_o$) respectively.

$$f_A = M \ln \left(\frac{p}{p_c} \right) + \left(\frac{q}{p} - \eta_o \right) = 0 \quad (24)$$

$$f_P = M \ln \left(\frac{p}{p_c} \right) - \left(\frac{q}{p} - \eta_o \right) = 0 \quad (25)$$

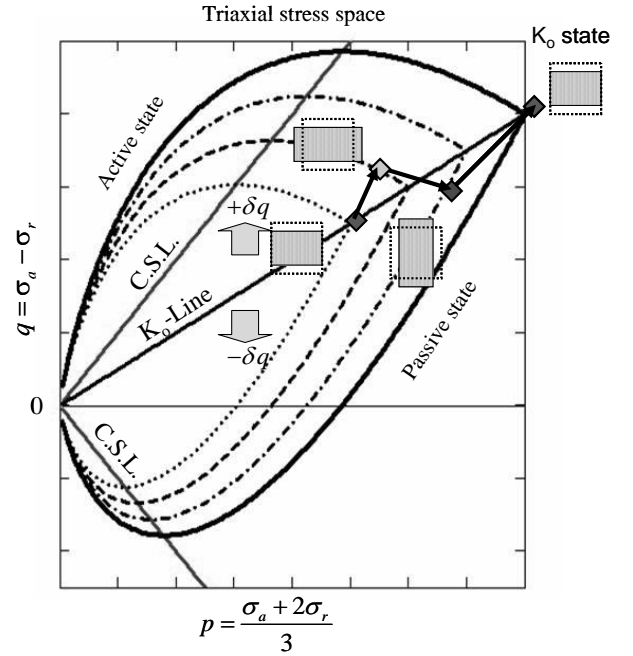


Fig. 1 Combination of active and passive loadings to succeed K_o state in which lateral strain is zero.

Stress derivatives of the yield loci respective to mean stress p , deviatoric stress q and hardening stress p_c are provided by Eqs.(26) and (27) while time derivatives are shown in Eqs. (30) and (31) which are equated to zero to satisfy consistency condition.

$$\begin{pmatrix} \frac{\partial f_A}{\partial p} & \frac{\partial f_P}{\partial p} \\ \frac{\partial f_A}{\partial q} & \frac{\partial f_P}{\partial q} \end{pmatrix} = \frac{1}{p} \begin{pmatrix} \beta_A & \beta_P \\ 1 & -1 \end{pmatrix}, \quad \begin{pmatrix} \frac{\partial f_A}{\partial p_c} \\ \frac{\partial f_P}{\partial p_c} \end{pmatrix} = \begin{pmatrix} -\frac{M}{p_c} \\ -\frac{M}{p_c} \end{pmatrix} \quad (26),(27)$$

$$\text{where } \beta_A = M - \eta, \quad \beta_P = M + \eta \quad (28),(29)$$

$$\dot{f}_A = \frac{\partial f_A}{\partial p} \dot{p} + \frac{\partial f_A}{\partial q} \dot{q} + \frac{\partial f_A}{\partial p_c} \dot{p}_c = 0 \quad (30)$$

$$\dot{f}_P = \frac{\partial f_P}{\partial p} \dot{p} + \frac{\partial f_P}{\partial q} \dot{q} + \frac{\partial f_P}{\partial p_c} \dot{p}_c = 0 \quad (31)$$

Let's activate the active and passive yield loci one by one to avoid involving with the intersection corner. Referring to flow rule, plastic volumetric and deviatoric strain rates emanated from the prescribed active stress are formulated into Eq. (32). Substitution of Eqs. (21), (26), (27) and (32) into Eq. (30) recasts the corresponding consistency parameters γ_A to Eq. (34).

$$\begin{cases} \dot{\epsilon}_v^p \\ \dot{\epsilon}_s^p \end{cases}_A = \gamma_A \begin{cases} \frac{\partial f_A}{\partial p} \\ \frac{\partial f_A}{\partial q} \end{cases}, \quad \begin{cases} \dot{\epsilon}_v^p \\ \dot{\epsilon}_s^p \end{cases}_P = \gamma_P \begin{cases} \frac{\partial f_P}{\partial p} \\ \frac{\partial f_P}{\partial q} \end{cases} \quad (32),(33)$$

$$\text{where } \gamma_A = \left(\dot{p} + \frac{\dot{q}}{\beta_A} \right) D, \quad \gamma_P = \left(\dot{p} - \frac{\dot{q}}{\beta_P} \right) D \quad (34),(35)$$

Using a relation of elastic and plastic strain decomposition shown in Eq. (36) and adopting stress relation under K_o -condition given by Eq.(8), the activated volumetric and deviatoric rate of strain under active stress condition driven by the prescribed rate of mean stress, can be achieved thru Eq. (37). By the similar way, those for passive stress condition also specified in Eqs.(31), (33), (35) and (38).

$$\begin{cases} \dot{\epsilon}_v \\ \dot{\epsilon}_s \end{cases} = \begin{cases} \dot{\epsilon}_v^e \\ \dot{\epsilon}_s^e \end{cases} + \begin{cases} \dot{\epsilon}_v^p \\ \dot{\epsilon}_s^p \end{cases} \quad (36)$$

$$\begin{cases} \dot{\epsilon}_v \\ \dot{\epsilon}_s \end{cases}_A = \begin{cases} \frac{1}{1-\Lambda} \\ \frac{\eta_o + \Lambda}{3\mu + (1-\Lambda)(M-\eta_o)} \end{cases} \begin{cases} \dot{p} \\ K \end{cases} \quad (37)$$

$$\begin{cases} \dot{\epsilon}_v \\ \dot{\epsilon}_s \end{cases}_P = \begin{cases} \frac{1}{1-\Lambda} \\ \frac{\eta_o - \Lambda}{3\mu - (1-\Lambda)(M+\eta_o)} \end{cases} \begin{cases} \dot{p} \\ K \end{cases} \quad (38)$$

2.3 Determination of K_o

Based on the fact that K_o condition existed on the discontinuous corner of the yield surface between active and passive yield loci, the combination of active and passive states can alternatively succeed K_o condition as illustrated by Fig. 1. The resulting strain rate successively developed by trespassing active and passive states is obtained in Eq. (39) as the sum of Eqs. (37) and (38). The ratio of deviatoric strain component to volumetric component of the combined strain rate is determined by Eq. (40) which is expected to be 2/3 if the K_o value suitable to the model is employed.

$$\begin{aligned} \begin{cases} \dot{\epsilon}_v \\ \dot{\epsilon}_s \end{cases} &= \begin{cases} \dot{\epsilon}_v \\ \dot{\epsilon}_s \end{cases}_A + \begin{cases} \dot{\epsilon}_v \\ \dot{\epsilon}_s \end{cases}_P \\ &= \begin{cases} \frac{1}{1-\Lambda} \\ \frac{\eta_o + \Lambda}{3\mu + (1-\Lambda)(M-\eta_o)(M+\eta_o)} \end{cases} \begin{cases} 2\dot{p} \\ K \end{cases} \end{aligned} \quad (39)$$

$$\frac{\dot{\epsilon}_s}{\dot{\epsilon}_v} = (1-\Lambda) \frac{\eta_o}{3\mu} + \Lambda \frac{\eta_o}{M^2 - \eta_o^2} \quad (40)$$

$$\frac{\eta_o}{M^2 - \eta_o^2} = \frac{2}{3} \quad (41)$$

$$\eta_o = \frac{\sqrt{9+16M^2} - 3}{4}, \quad K_o = \frac{15 - \sqrt{9+16M^2}}{6 + 2\sqrt{9+16M^2}} \quad (42), (43)$$

$$M = \frac{6 \sin \phi}{3 - \sin \phi} \quad (44)$$

$$K_o = 0.44 + 0.42 \frac{I_p}{100} \quad (45)$$

$$\sin \phi = 0.81 - 0.233 \log I_p \quad (46)$$

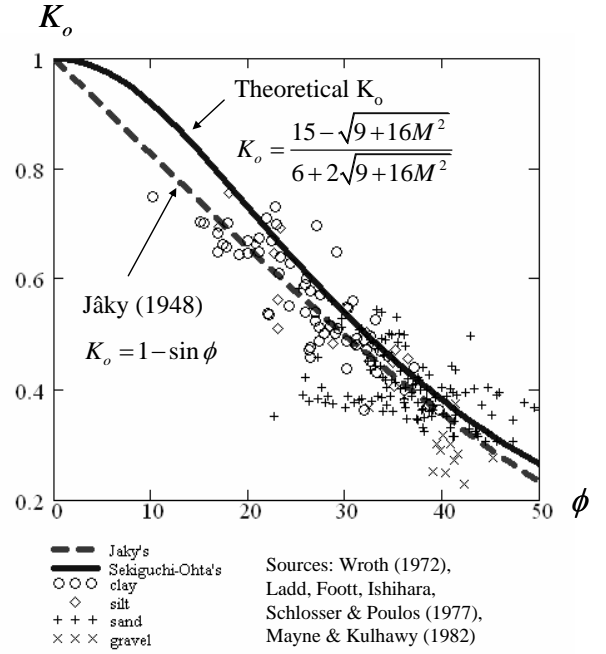


Fig. 2 Relation between K_o and ϕ

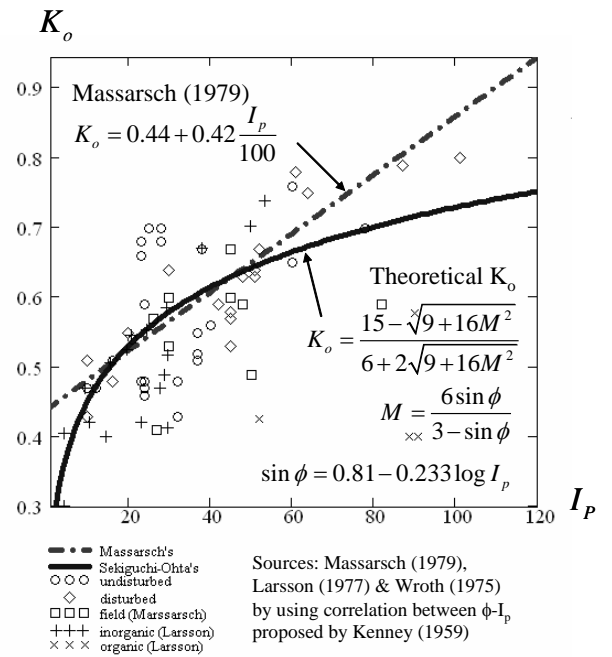


Fig. 3 Relation between K_o and I_p

Substituting the relation derived in Eq. (17) into Eq. (40) and replacing the strain ratio on the left-hand side of Eq.(40) to 2/3, under this criterion, Eq. (40) can be reduced to Eq. (41) for solving the unknown η_0 . The theoretical K_0 expression can be evaluated analytically as the expression solely related to M shown by Eq. (42) which can be further converted to K_0 using the relation shown in Eq. (8). In Fig. 2, the comparison of the derived expression with the famous semi-empirical relationship proposed by Jaky (1948) using a relation between M and the internal frictional angle ϕ given in Eq. (44) shows a good agreement. Besides, In Fig. 3, the empirical correlation between K_0 and plasticity index I_p proposed by Massarsch (1979) in Eq.(45) can be related to the internal friction angle using the empirical relation proposed by Kenny (1959) as indicated Eq.(46). The derived expression is acceptably supported by the available published experimental data of various kinds of soils by summarizing Figs. 2 and 3 to Fig. 4.

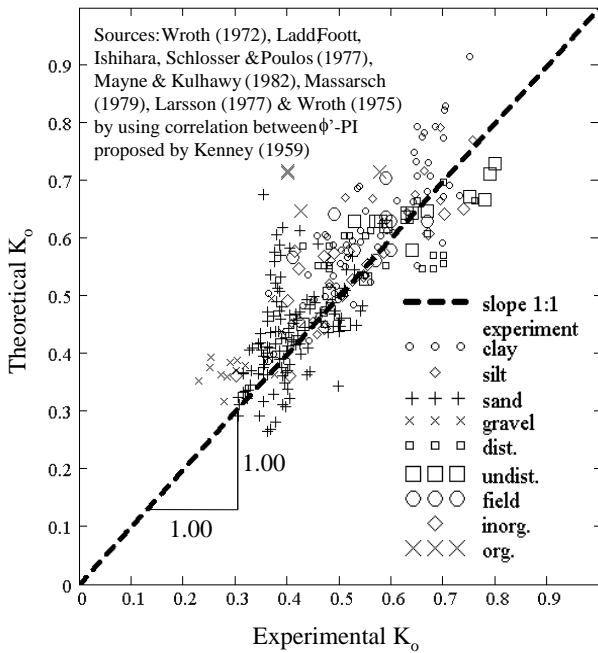


Fig. 4 Theoretical and experimental values of K_0 compiled from published sources

3 NUMERICAL ILLUSTRATION

The slight interruption is undertaken upon numerically perturbing the state of stress at the K_0 condition by small amount of balanced horizontal stress increments can activate active and passive states. The resulting successive stress condition is, therefore, kept tracing and fluctuating along the K_0 -consolidation axis whilst increasing a consolidated volume. Thus, the numerical illustration can be carried out simply by FEM. The continuum tangent modulus in generalized stress employed in FEM is explained in Appendix.

3.1 Loading and Boundary Conditions

A single rectangular element under fully-drained axi-symmetric condition with material properties listed in Table 1 is subject to a series of applying passive and active loadings in corresponding to a constant incremental vertical stress. The incremental horizontal stress at K_0 state is obtained by a multiplication of K_0 value to an

incremental vertical stress. A disturbance δ in proportional to K_0 value (herein applying $\delta=1/2$) is added to K_0 value to initiate passive load exerting to the element. In the other hand, to vanish passive state for the next loading step, a similar amount of disturbance is subtracted to K_0 value to initiate active load. It is clear that the sum of horizontal stresses for both passive and active loads can finally balance the horizontal stress back to K_0 state as envisaged in Fig. 5.

7 cases of the selected K_0 values ranging from 0.50 to 0.80 are employed along with other common values of material parameters. Poisson's ratio is associated to each input K_0 value by the relation given in Eq.(18). Boundary condition is defined in the way to allow horizontal displacement and vertical displacement in accordance with horizontal loadings and vertical loadings respectively. The FEM program used in this study is DACSAR (Iizuka & Ohta, 1987) which has been developed for geotechnical engineering practices in Japan more than 20 years. To refine the quality of computation, the respective loading steps are divided into 100 sub-steps.

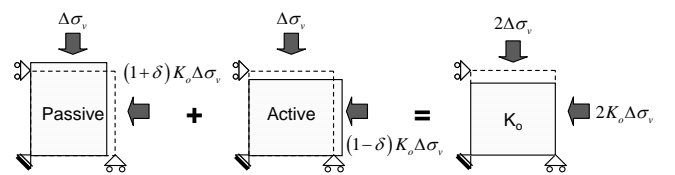


Fig. 5 Diagram of loading conditions (in case of 2 steps).

Table 1 Material parameters

Parameter	Description	Value
D	Coefficient of dilatancy	0.1128
Λ	Irreversibility ratio	0.825
M	Critical state parameter	1.00
K_0	Coefficient of earth pressure (NC)	0.50~0.80
K_i	Coefficient of earth pressure (in-situ)	0.50~0.80
ν	Poisson's ratio	$K_0/(1+K_0)$
λ	Compression index	0.342
e_0	Void ratio at σ'_{vo}	1.50
σ'_{vo}	Preconsolidation pressure (kN/m ²)	100
σ'_{vi}	Overburden pressure (kN/m ²)	75

3.2 Computational Results

Fig. 6 shows the resulting stress paths in p - q stress space for each case of input K_0 values. Owing to the initial OCR = 4/3, it is evident that the stress path of all cases start inside elastic region and fluctuate between active and passive states while progressing across yield surface to elasto-plastic region thoroughly by the averaged slope governed by the input values of K_0 . During elastic state, despite of zigzagging appearance, averaged strain ratio $\Delta\epsilon_s/\Delta\epsilon_v$ of all cases remains constant at 2/3, signifying zero lateral strain. However, under process of normal consolidation, it tends to divert from 2/3 as observed in Fig. 7, pointing out that K_0 condition is violated. However, the ratio is likely to remain at 2/3 if the suitable input value of K_0 is chosen. To investigate the suitable input value of K_0 , the chart plotted between η_0 against average of strain ratio $\Delta\epsilon_s/\Delta\epsilon_v$ obtained from Fig.7 by linearization is described in Fig.8.

There is a definite value of η_0 which can maintain the averaged strain ratio at 2/3, hence, agreeing with K_0 condition either

loading/unloading on both elastic and elasto-plastic regions. Here, it reveals that this unique value is $\eta_o=0.50$ (or $K_o=0.625$), conforming with Eq.(42) (or Eq.(43)) for $M=1$. Moreover, it is obvious that the equation of curve in Fig.8 follows Eq.(40). The relation at $\eta_o=0.75$ seems to distract from the equation because the strain ratio is likely to be a curved line rather than a linear line as observed in Fig. 7.

To verify the FEM result, the e-log(p) curve is drawn in Fig. 9 to confirm swelling and compression index obtained from the computation with the input parameters. It is interested to find out that without considering Koiter's flow rule (Koiter, 1953) to the corner of the Sekiguchi-Ohta model, the FEM result of virgin K_o -consolidation cannot achieve a correct compression index, however, the calculation done by combination of active and passive loadings can achieve stress-strain responses correctly.

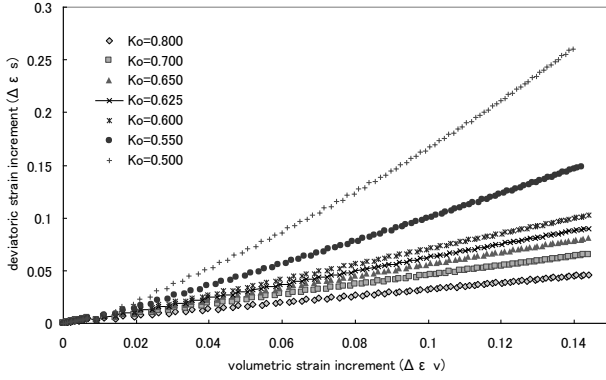


Fig. 6 Stress paths obtained from calculation for each K_o value.

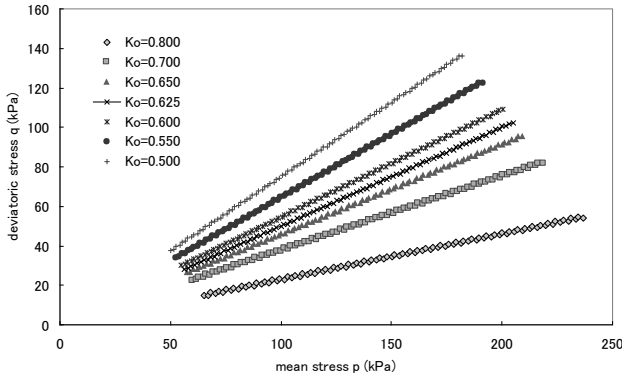


Fig. 7 Strain paths obtained from calculation for each K_o value.

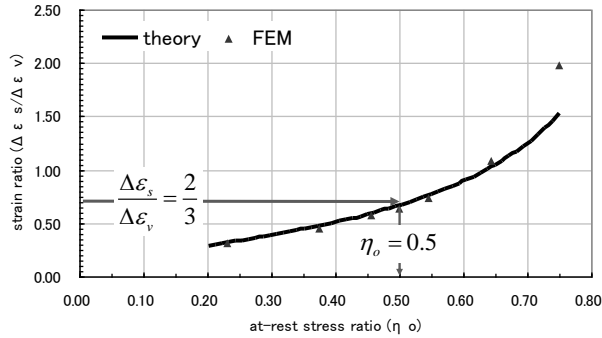


Fig. 8 Determination of suitable η_o on the curve at $\Delta\epsilon_s/\Delta\epsilon_v=2/3$

4 CONCLUSION

The theoretical K_o for normally consolidated soils expressed as the function of critical state parameter M was derived for the Sekiguchi-Ohta model. Though the proposed method is not performed by applying the actual K_o -consolidation loading, it can suggest that the stress-strain responses regulated by the Sekiguchi-Ohta model can be more or less inaccurate if incorrect K_o is used in some specific problem like the illustration demonstrated in this paper. The benefit gained from this study is that the material parameter for the model can be reduced by one. However, this paper has not yet systematically investigated the qualitative effect of K_o value involving in the predicted performance of numerical simulations, thus, this topic is still opened for further examination.

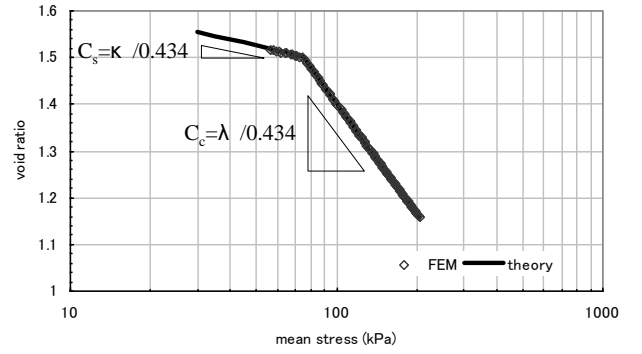


Fig. 9 Verification of consolidation process by e-log(p) curve.

ACKNOWLEDGMENTS

The authors are grateful to Dr. Shintaro Ohno, Ritsumeikan University for helpful discussions on the subject matter which aided the development of the ideas proposed in this paper.

APPENDIX

The inviscid form of the Sekiguchi-Ohta model for generalized stresses are shown in Eq.(47). The continuum tangent modulus employed by FEM can be derived as follows:

$$f = M \ln \left(\frac{p}{p_c} \right) + \frac{\bar{q}}{p} = 0 \quad (47)$$

where

$$p = \frac{1}{3} \boldsymbol{\sigma} : \mathbf{1}, \quad p_c = \frac{1}{3} \boldsymbol{\sigma}_c : \mathbf{1}, \quad \mathbf{s} = \boldsymbol{\sigma} - p \mathbf{1} \quad (48),(49),(50)$$

$$\mathbf{s}_c = \boldsymbol{\sigma}_c - p_c \mathbf{1}, \quad \boldsymbol{\eta}_c = \frac{\mathbf{s}_c}{p_c}, \quad \bar{\mathbf{s}} = \mathbf{s} - p \boldsymbol{\eta}_c \quad (51),(52),(53)$$

$$q_c = \sqrt{\frac{3}{2} \mathbf{s}_c : \mathbf{s}_c}, \quad \bar{q} = \sqrt{\frac{3}{2} \bar{\mathbf{s}} : \bar{\mathbf{s}}} \quad (54),(55)$$

Stress derivatives of yield function

$$\frac{\partial f}{\partial \boldsymbol{\sigma}} = \frac{\partial f}{\partial p} \frac{\partial p}{\partial \boldsymbol{\sigma}} + \frac{\partial f}{\partial \bar{q}} \frac{\partial \bar{q}}{\partial \boldsymbol{\sigma}} = \frac{1}{p} \left\{ \frac{1}{3} \beta \mathbf{1} + \sqrt{\frac{3}{2}} \bar{\mathbf{n}} \right\} \quad (56)$$

where

$$\beta = M - \frac{\bar{q}}{p} - (\mathbf{n}_c : \bar{\mathbf{n}}) \eta_o \quad (57)$$

$$\mathbf{n}_c = \frac{\mathbf{s}_c}{\|\mathbf{s}_c\|} = \sqrt{\frac{3}{2}} \frac{\mathbf{s}_c}{q_c}, \quad \bar{\mathbf{n}} = \frac{\bar{\mathbf{s}}}{\|\bar{\mathbf{s}}\|} = \sqrt{\frac{3}{2}} \frac{\bar{\mathbf{s}}}{\bar{q}} \quad (58),(59)$$

Time derivatives of the yield function is expressed by,

$$\dot{f} = \frac{\partial f}{\partial \boldsymbol{\sigma}} : \dot{\boldsymbol{\sigma}} + \frac{\partial f}{\partial p_c} \dot{p}_c \equiv 0 \quad (60)$$

where

$$\frac{\partial f}{\partial p_c} = -\frac{M}{p_c}, \quad \dot{p}_c = \frac{p_c}{MD} \dot{\varepsilon}_v^p \quad (61),(62)$$

$$\dot{\boldsymbol{\varepsilon}}^p = \gamma \frac{\partial f}{\partial \boldsymbol{\sigma}}, \quad \dot{\varepsilon}_v^p = \mathbf{1} : \dot{\boldsymbol{\varepsilon}}^p \quad (63),(64)$$

$$\gamma = D \frac{\frac{\partial f}{\partial \boldsymbol{\sigma}} : \dot{\boldsymbol{\sigma}}}{\frac{\partial f}{\partial \boldsymbol{\sigma}} : \mathbf{1}} \quad (65)$$

Alternatively,

$$\gamma = \frac{\frac{\partial f}{\partial \boldsymbol{\sigma}} : \mathbf{c}^e : \dot{\boldsymbol{\varepsilon}}}{\frac{\partial f}{\partial \boldsymbol{\sigma}} : \mathbf{c}^e : \frac{\partial f}{\partial \boldsymbol{\sigma}} + \frac{\partial f}{\partial \boldsymbol{\sigma}} : \frac{\mathbf{1}}{D}} \quad (66)$$

Incremental stress-strain relation is described below,

$$\dot{\boldsymbol{\varepsilon}} = \dot{\boldsymbol{\varepsilon}}^e + \dot{\boldsymbol{\varepsilon}}^p = \mathbf{c}^{ep-1} : \dot{\boldsymbol{\sigma}} \quad (67)$$

where

$$\dot{\varepsilon}_v = \mathbf{1} : \dot{\boldsymbol{\varepsilon}}, \quad \dot{\boldsymbol{\varepsilon}}_d = \mathbf{A} : \dot{\boldsymbol{\varepsilon}}, \quad \dot{\varepsilon}_s = \sqrt{\frac{2}{3}} \dot{\boldsymbol{\varepsilon}}_d : \dot{\boldsymbol{\varepsilon}}_d \quad (68),(69),(70)$$

$$\mathbf{c}^{ep-1} = \mathbf{c}^{e-1} + D \frac{\frac{\partial f}{\partial \boldsymbol{\sigma}} \otimes \frac{\partial f}{\partial \boldsymbol{\sigma}}}{\frac{\partial f}{\partial \boldsymbol{\sigma}} : \mathbf{1}} \quad (71)$$

$$\mathbf{c}^{ep} = \mathbf{c}^e - \frac{\mathbf{c}^e : \frac{\partial f}{\partial \boldsymbol{\sigma}} \otimes \frac{\partial f}{\partial \boldsymbol{\sigma}} : \mathbf{c}^e}{\frac{\partial f}{\partial \boldsymbol{\sigma}} : \mathbf{c}^e : \frac{\partial f}{\partial \boldsymbol{\sigma}} + \frac{1}{D} \frac{\partial f}{\partial \boldsymbol{\sigma}} : \mathbf{1}} \quad (72)$$

$$\mathbf{c}^e = K \mathbf{1} \otimes \mathbf{1} + 2G \mathbf{A} \quad (73)$$

$$\mathbf{c}^{e-1} = \frac{1}{9K} \mathbf{1} \otimes \mathbf{1} + \frac{1}{2G} \mathbf{A} \quad (74)$$

Related tensors are defined below,

$$\mathbf{e}^{<i>}. \mathbf{e}^{<j>} = \delta_{ij}, \quad \mathbf{1} = \delta_{ij} \mathbf{e}^{<i>} \otimes \mathbf{e}^{<j>} \quad (75),(76)$$

$$\mathbf{1} \otimes \mathbf{1} = \delta_{ij} \delta_{kl} \mathbf{e}^{<i>} \otimes \mathbf{e}^{<j>} \otimes \mathbf{e}^{<k>} \otimes \mathbf{e}^{<l>} \quad (77)$$

$$\mathbf{I} = \frac{1}{2} [\delta_{ik} \delta_{jl} + \delta_{il} \delta_{jk}] \mathbf{e}^{<i>} \otimes \mathbf{e}^{<j>} \otimes \mathbf{e}^{<k>} \otimes \mathbf{e}^{<l>} \quad (78)$$

$$\mathbf{A} = \mathbf{I} - \frac{1}{3} (\mathbf{1} \otimes \mathbf{1}) \quad (79)$$

where $\delta_{ij} = \begin{cases} 1 & \text{if } i = j \\ 0 & \text{if } i \neq j \end{cases}$ is Kronecker delta

REFERENCES

- Iizuka, A. & Ohta, H. 1987. A determination procedure of input parameters in elasto-viscoplastic finite element analysis, *Soils and Foundation* 27, No.3: 71-87.
- Jáky, J. 1948. Pressure in silos. *Proc. 2nd ICSMFE*, Rotterdam, the Netherland, Vol. 1: 103-107.
- Kenney, T.C. 1959. Discussion of Geotechnical. Properties of Glacial Lake Clays by Wu, T.H., J. *Soil Mech. Found. Div. ASCE* 85, No. SM3: 67-79.
- Koiter, W.T. 1953. Stress-strain relations, uniqueness and variational theorems for elastic-plastic materials with a singular yield surface, *Quart. Appl. Math.* 11: 350-354.
- Larsson, R. 1977. Basic behaviour of Scandinavian soft clays, *Swedish Geotechnical Institute, Linköping, Report* 4.
- Ladd, C.C., Foott, R., Ishihara, K., Schlosser, F., & Poulos, H.G. 1977. Stress-deformation and strength characteristics, *Proc. 9th ICSMFE*, Tokyo, vol. 2: 421-94.
- Massarsch, K.R. 1979. Lateral earth pressure in normally consolidated clay, *Proc. 7th ECSMFE*, vol. 2: 245-49.
- Mayne, P.W. & Kulhawy, F.H. 1982. Ko-OCR relationships in soil, *J. Geotech. Engng., ASCE* 108, No. GT6: 851-872.
- Ohta, H. & Hata, S. 1971. On the state surface of anisotropically consolidated clays, *Proc. of JSCE 196*: 220-227.
- Pipatpongsa, T., Ohta, H., Kobayashi, I. and Iizuka, A. 2001. Dependence of Ko-value on effective internal friction angle in regard to the Sekiguchi-Ohta model, *Proc. of 36th Japanese Nat. Conf. on Geotech. Engng*: 937-938.
- Pipatpongsa, T., Iizuka, A., Kobayashi, I. & Ohta, H. 2002. FEM formulation for analysis of soil constitutive model with a corner in the yield surface, *Journal of Structural Engineering, JSCE Vol.48A*: 185-194.
- Pipatpongsa, T., Iizuka, A. & Ohta, H. 2007. Coefficient of earth pressure at rest based on critical state model. (*in prep.*).
- Roscoe, K.H., Schofield, A.N & Thurairajah, A. 1963. Yielding of clays in state wetter than critical, *Géotechnique* 13, No.3: 211-240.
- Roscoe, K.H. & Burland, J.B. 1968. On the generalised stress-strain behavior of wet clay, *Engineering Plasticity*, Cambridge University Press: 535-609.
- Schofield, A. & Wroth, P. 1968. *Critical State Soil Mechanics*, McGRAW-HILL
- Sekiguchi, H. & Ohta, H. 1977. Induced anisotropy and time dependency in clays, *Proc. 9th ICSMFE*, Tokyo: 229-239.
- Wood D.M. 1990. Soil behavior and Critical state soil mechanics, *Cambridge University Press*.
- Wroth, C.P. 1975. In-situ measurement of initial stresses and deformation characteristics, *Proc. Specialty Conf. On In-Situ Measurement of Soil Properties*, Raleigh, North Carolina (New York: ASCE), vol. 2: 181-230.
- Wroth, C.P. 1972. General theories of earth pressure and deformation, *Proc. 5th ECSMFE*, Madrid, vol. 2: 33-52.